CRESST

W. Seidel[1],[a], G. Angloher[a], M. Bauer[c], I. Bavykina[a], A. Brown[e], C. Bucci[d],
C.Ciemniak[b], G. Deuter[c], F. von Feilitzsch[b], D. Hauff[a], S. Henry[e], P. Huff[a], C.Isaila[b],
J. Jochum[c] M. Kiefer[a], M. Kimmerle[c], R. Kleindienst[a], H. Kraus[e], Q. Kronseder[a],
J.C.Lanfranchi[b], V. B. Mikhailik[e], F. Petricca[a], S. Pfister[b], W. Potzel[b], F. Pröbst[a],
S.Roth[b], K. Rottler[c], C. Sailer[b], K. Schäffner[a], J. Schmaler[a], S. Scholl[c],
M.vonSivers[b], L. Stodolsky[a], C. Strandhagen[c], R. Strauß[b], I. Usherov[c]

[a] *Max Planck Institut für Physik*
 Föhringer Ring 6, D-80805 München, Germany
 E-mail: `seidel@mppmu.mpg.de`

[b] *Technische Universitä t München, Physik-Department E15,*
 D-85747 Garching, Germany

[c] *Eberhard-Karls-Universität Tübingen,*
 D-72076 Tübingen, Germany

[d] *INFN, Laboratori Nazionali del Gran Sasso,*
 I-67010 Assergi, Italy

[e] *Department of Physics, University of Oxford,*
 Oxford OX1 3RH, United Kingdom

[1]   Speaker

1. Introduction

There is strong evidence for the existence of dark matter on all astronomical scales, and the history of the universe is difficult to reconstruct without it. Despite this persuasive indirect evidence for its existence, the direct detection of dark matter remains one of the outstanding experimental challenges of present-day physics.

A plausible candidate for the dark matter is the Weakly Interacting Massive Particle (WIMP) and it is possible that it can be detected by laboratory experiments. In particular, cryogenic methods which are well adapted to the small energy deposits anticipated can be employed. Supersymmetry provides a well-motivated WIMP candidate in the form of the Lightest Supersymmetric Particle. WIMPs are expected to be gravitationally bound in a roughly isothermal halo around the visible part of our galaxy with a density of about 0.3 GeV/cm^3 at the position of the Earth.

Interaction with ordinary matter is expected via elastic scattering off nuclei. This elastic scattering can occur via coherent (spin-independent) and spin-dependent interactions. For the coherent case, a factor A^2 is expected in the cross-section, favoring heavy nuclei to be used as a target. Due to this factor, in a composite target like $CaWO_4$, the total scattering rate is dominated by recoils of tungsten. However, in a real experiment with a finite energy threshold, also the other nuclei can be relevant, as tungsten recoils may not be energetic enough to be detected. Fig.1 shows the contribution of the three types of nuclei in $CaWO_4$ to a recoil spectrum measured in the energy interval from 10 to 40 keV. WIMPs with a mass below 10GeV would not be able to produce visible tungsten recoils above threshold, most of the observable recoils would be on oxygen and some on Ca. For a small range of WIMP masses above 10GeV, Ca is most important while for WIMP masses above 20 GeV tungsten recoils dominate.
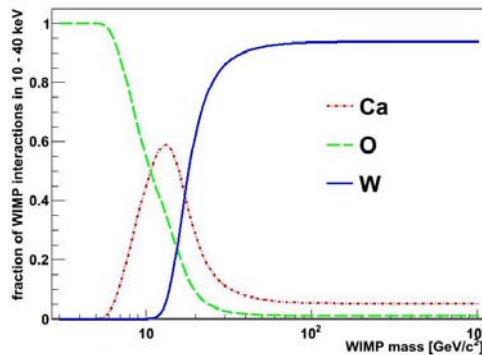
Figure 1: Relative contribution of the three types of recoil nuclei in $CaWO_4$ as a function of the WIMP mass. The calculation assumes that recoils above 10 keV can be measured.

Most methods for direct detection measure the recoil energy via the ionization or scintillation caused by the recoiling nucleus. This leads to certain limitations connected with the low ionization or scintillation efficiency of the slow recoil nuclei. The cryogenic detectors developed for CRESST measure the deposited energy calorimetrically, independent of the type of interaction. When such a calorimetric measurement of the deposited energy is combined with a measurement of scintillation light, an extremely efficient discrimination of the nuclear recoils from radioactive background can be obtained and the type of recoiling nucleus can be determined in a multi atomic target.

2. Detection Principle
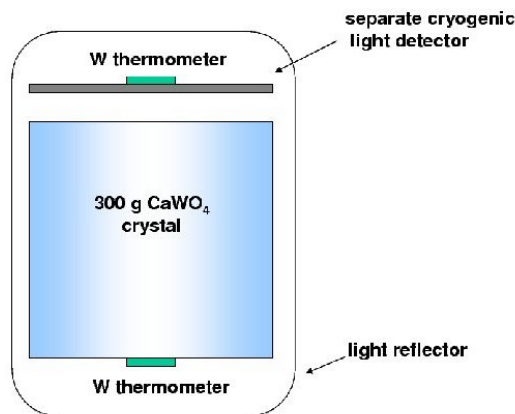
Figure 2: Schematic representation of the detector for simultaneous phonon and light measurement. It consists of two separate cryogenic detectors enclosed in a highly reflective housing, read out by tungsten superconducting phase-transition thermometers. This concept allows a very efficient discrimination of nuclear recoil signals from the dominant radioactive β- and γ-backgrounds.

A low-temperature calorimeter consists of a target crystal with a superconducting phase transition thermometer on its surface. The thermometer is made of a tungsten film evaporated onto the target crystal. Its temperature is stabilized within the transition from the superconducting to the normal conducting state, which occurs at temperatures of about 10mK. A typical width of the transition is about 1 mK. A small temperature rise, e.g. from a WIMP-nucleus scattering event, of typically some μK, leads to an increase of resistance of some $\mu\Omega$, which is measured with a SQUID (**S**uperconducting **Qu**antum **I**nterference **D**evice). A weak thermal coupling of the thermometer to the heat bath restores the equilibrium temperature again after an interaction.

In CRESST-II, 300 g scintillating $CaWO_4$ crystals are used as target. In these crystals a particle interaction creates mostly phonons which are detected by the phase transition thermometer. In addition, a small fraction of 1 to 2% of the deposited energy is transformed into scintillation light and detected in a separate cryogenic detector, optimized for light detection.

Fig.2 shows a scheme of such a detector module, consisting of the target crystal and its light detector
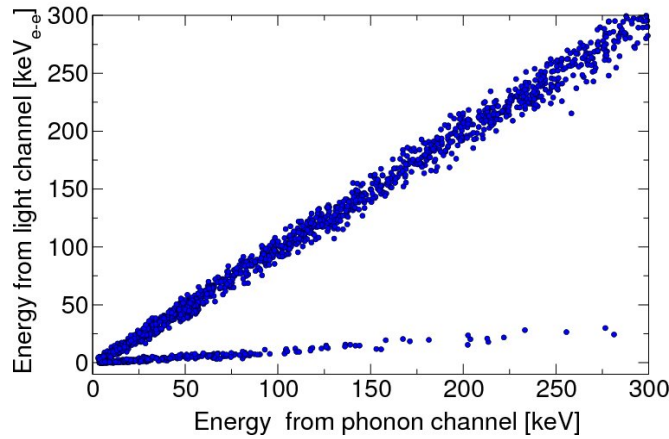
Figure 3: Coincident detection of phonons and scintillation light with a 300 g CaWO$_4$ detector. The upper band of events is due to interaction of electrons and gammas in the CaWO$_4$ crystal. The lower band with less light is from nuclear recoils caused by a neutron source. Data are from a neutron test of in the 2009/2010 run

The important advantage of simultaneous measurement of phonons and scintillation light is that it offers a very efficient suppression of the radioactive background down to low recoil energies of about 10 keV. The phonon signal measures the energy deposited in the scintillating target crystal with high accuracy, while the amplitude of the corresponding light signal depends on the type of interaction. Nuclear recoils from WIMP or neutron scattering events emit substantially less scintillation light than fully ionizing interactions, e.g. γ- or β- interactions. As the overwhelming part of the background consists of β- and γ-interactions, this phonon/light technique provides a very effective method of background suppression. Fig.3 illustrates this detection method with a neutron test.

For a particular class of background events, it is desirable that all surfaces inside the detector housing are scintillating. These are events from surface alpha decays, an example of which is shown in Fig.4.
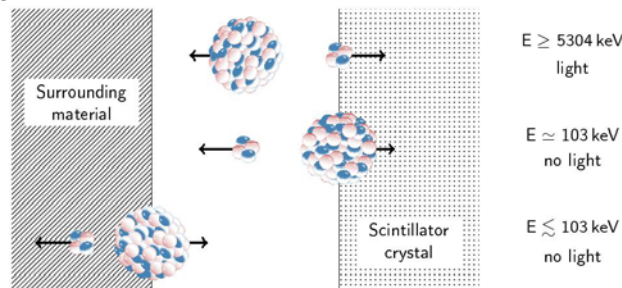
Figure 4: Illustration of background events due to surface contaminations with [210]Po.

The main source of such backgrounds is the isotope [210]Po which can sit on or be implanted in the surfaces of detectors and surrounding material. These atoms decay to [206]Pb, under the emission of 5.4 MeV α-particle and with a recoiling lead nucleus with 105 keV of kinetic energy. It can happen that only the recoiling nucleus hits the target crystal and deposits its energy there while the α-particle escapes. Due to its high mass, such a lead recoil will be indistinguishable from a tungsten recoil event and thus can mimic a WIMP. In case the original polonium atom was sitting on the surface of the crystal or even implanted in it (the upper case in Fig.4, at least the full energy of the daughter nucleus plus a possible contribution from the escaping α-particle will be deposited in the crystal and the event is thus above the energy range relevant for WIMP search. However, in case the polonium atom was implanted in one of the surrounding surfaces, the daughter nucleus can lose part of its energy already on the way to the crystal and thus appear in the energy range of interest (lower case in Fig.4). However, if the surrounding surfaces are scintillating, the escaping α-particle produces additional scintillation light when hitting those materials. Hence the event will no longer appear in the signal region.

The phonon/light technique is firstly capable of distinguishing β/γ-backgrounds from nuclear recoils, and further to some extent even of distinguishing which type of nucleus is recoiling in the $CaWO_4$ crystal. This latter point would be very useful in verifying a possible positive dark matter signal via its dependence on different nuclei (something not possible for many other types of dark matter detectors). For these reasons, the CRESST collaboration has undertaken extensive studies by various methods of the "quenching factor" (relative light output) for different recoiling nuclei. [1] [2].

3.The CRESST Setup in Gran Sasso

The central part of the CRESST installation at Gran Sasso is the cryostat, surrounded by active and passive shielding, as sketched in Fig.5. A 1.5m long cold finger connects the detectors, which are mounted inside a radiopure cold box, with the mixing chamber of the dilution refrigerator. Two internal cold shields consisting of lead with a low intrinsic radioactivity are attached to the mixing chamber and to a thermal radiation shield at liquid N_2 temperature, respectively, in order to block any line-of-sight from the non-radio-pure parts of the dilution refrigerator to the detectors inside the cold box. An extensive passive shielding of 15 cm of low-background copper and 20 cm of lead surrounds the cold box and serves to shield radioactivity from the surrounding rock. The entire shielding is enclosed inside a gas-tight radon box that is flushed with N_2 gas and maintained at a small overpressure. The radon box is surrounded by plastic scintillator panels serving as a μ-veto. The whole setup is enclosed in a neutron shield consisting of 40 cm of polyethylene.
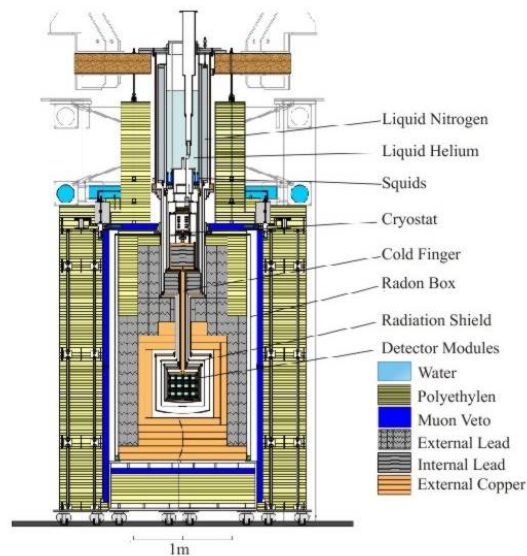
Figure5: ^{3}He-^{4}He dilution refrigerator, low background detector environment, and the shielding as upgraded for CRESST-II.

4. Present run 2009/2010

Since a scintillator coating of the clamps holding the crystals is still under development, all detector modules were equipped with bare metallic clamps.

The first cool-down in April 2009 was interrupted by the earth quake in the L'Aquila region. After repairing some of the detector modules, the present run finally started in May 2009. 10 complete detector modules were running one week after start including three crystals with a glued thermometer. One of them is a $ZnWO_4$ crystal, which, compared to $CaWO_4$, has a higher light output at low temperatures. An energy calibration of all modules with a 122 keV gamma line from a ^{57}Co source was performed before starting the dark matter run. Generally, the detectors were running very stably, with occasional disturbances due to the continuing seismic activity in the first months of the run.

4.1 Neutron Test

To directly test the response of the system to nuclear recoils a neutron test was carried out in May 2010. The test allows to check the principle of identifying the recoiling nucleus via the light yield. Above a recoil energy of ~10 keV, simulations show that the spectrum for neutron scattering on $CaWO_4$ is dominated by oxygen recoils.

For this test, a weak (~10 neutrons/second) ^{241}Am-Be neutron source was placed at two different positions inside the neutron shielding. Before reaching the detectors, neutrons had to pass the 20 cm of lead and 15 cm of copper of the shielding. Data of one of the detector modules are shown in Fig.6. Below the upper line in Fig.6, 90% of the oxygen recoils are expected and 10% should lie below the lower line. The lines were calculated from the energy

resolution of the light channel and the known quenching factor of 9.6 for oxygen recoils. The good agreement of the data with the prediction supports the use of this method to identify also calcium and tungsten recoils in the dark matter analysis. Highlighted events in Fig.6 are within the energy range of the signal region to be discussed later. The few events above 47keV between the electron and nuclear recoil bands can be understood as double scattering: An inelastic neutron scattering where the tungsten nucleus is excited to a gamma-emitting level, and an elastic neutron-oxygen scattering. All other detector modules show a similarly excellent nuclear recoil discrimination.
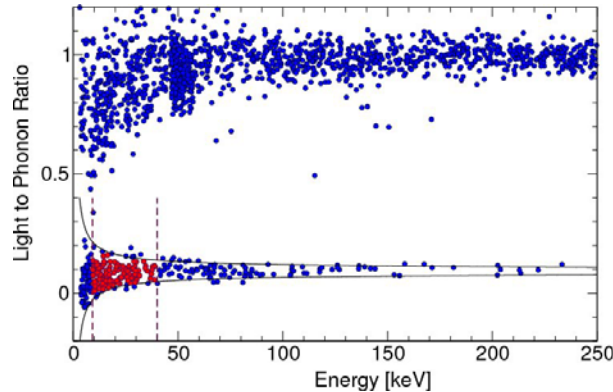
Figure 6: Event distribution in the energy light yield plane, measured with detector module ch51/52 with an Am-Be neutron neutron source placed outside the Pb and Cu shielding. Below the upper and lower curve 90% and 10% of the oxygen recoils are expected respectively. The curves were calculated from the known quenching factor for oxygen and the energy resolution of the light detector.

4.2 Results

About 400 kg-days of the recorded data has been analyzed at the time of this writing. Fig.7 shows data of detector module ch5/6 recorded from September 2009 to May 2010. The band where oxygen recoils are expected is shown in magenta. There is a clear population of events in this oxygen band. The area where tungsten recoils are expected is shown in brown. Below about 45 keV, oxygen and tungsten bands partially overlap. Larger red circles identify oxygen recoils in the signal region, a single tungsten recoil in the signal region is shown in dark dark violet.
Since the clamps holding the crystal are not covered with scintillator in this run, events from degraded alpha particles appear in the yellow alpha-band. Additionally, recoiling ^{206}Pb nuclei from ^{210}Po alpha decays can be seen in the tungsten band at an energy of about 100 keV, with some tail extending towards lower energies. The quenching factors of tungsten and lead are too similar to distinguish both types of recoils. The tail seems to end around 65 keV. Apart from these events, the tungsten band is quite empty. However, some leakage of such recoil nuclei from alpha decays into the signal energy range of the tungsten band can not be completely excluded. The following discussion will therefore concentrate on events in the oxygen band, which do not suffer much from this potential contamination. Our still ongoing analysis

concentrates on identifying or excluding mechanisms which might contribute to events in the oxygen band.
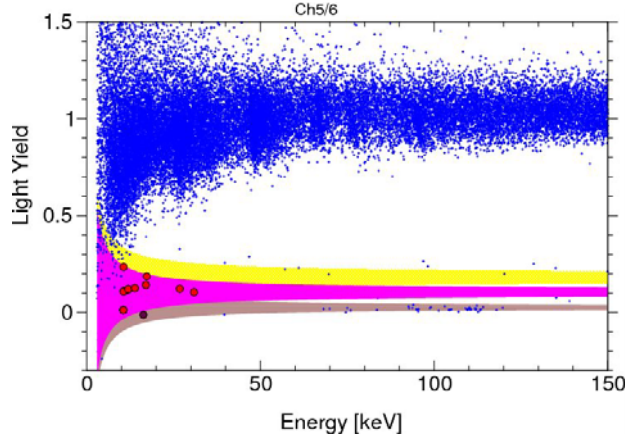
Figure 7: Data of detector module ch5/6. The magenta colored area is the oxygen band, where 80% of the oxygen recoils are expected (90% below the upper and 10% below the lower end). Tungsten and alpha bands are shown in brown and yellow.

Events in the oxygen band may be due to neutrons or some leakage of alpha backgrounds, or, when all other possibilities can be ruled out with high confidence, induced by low mass WIMPs.

Detector	$E_{0.1}$ [keV]	not coincident	coincident
Ch05	12.35	5	0
Ch20	11.85	2	0
Ch29	11.65	4	1
Ch33	15.55	2	1
Ch43	15.55	4	1
Ch45	19.15	2	0
Ch47	17.35	4	0
Ch51	9.65	5	0
Ch55	22.25	3	0
total		**32**	**3**

Table 1: Number of oxygen recoil events observed in the signal energy range ($E_{0.1}$ to 40keV) of each detector. Some recoils were observed in coincidence in more than one detector module. The total exposure is about 400 kg-days.

For each detector we define a useful signal energy range for the oxygen recoils. The lower energy limit $E_{0.1}$ is chosen such that a leakage of 0.1 gamma events is expected in the signal

energy range, while the same upper limit of 40 keV is chosen for all detectors. When the WIMP is massive enough to produce oxygen recoils much above 40 keV, the recoil spectrum should be totally dominated by tungsten recoils. As this is not observed, it motivates the choice of 40 keV as upper energy limit. Table 1 lists the number of events observed in the oxygen signal region of each detector. In total, 32 single oxygen recoil events were observed in ~400 kg·days. The 3 coincident recoils, also listed in Table1, are in fact two events, both triple coincidences. The first event consists of two oxygen recoils in the signal energy range of two detector modules, together with a 1.8 MeV gamma in a third detector, while the second coincident event is an oxygen recoil in the signal energy range of one detector, a 33 keV gamma in a second detector, together with an 1.16 MeV gamma in a third one. Coincident oxygen-oxygen recoils like in the first of the two coincident events can only come from neutrons. However, when there are coincident neutron events, there should be also single scatters which are indistinguishable from WIMP scatters off oxygen.

4.2.1 Estimation of Neutron Background

Neutrons from alpha-n reactions and spontaneous fissions in the surrounding rock should be sufficiently shielded by the 45 cm of polyethylene. Indeed, Monte Carlo simulations would give a rate of only ~10^{-5}/kg·day [3]. Fast neutrons produced by high energy muons in the rock are more difficult to estimate. Monte Carlo studies would give a rate of ~1 event/400 kg-days [4]. With good probability fast neutrons should multiply in the Pb/Cu shielding, and a higher level of coincidences may be expected for such neutrons compared to neutrons from spontaneous fission or alpha-n reactions. To learn more about the origin of the observed 2 coincident events in the data, we compare their event structure with that of oxygen recoils tagged by the muon veto and with that of oxygen recoils measured in the neutron test. In total, we have observed 25 muon coincident events with an oxygen recoil in the signal energy range in at least one of the detector modules. 19 of these coincident events are from through going muons, i.e. the muon was registered in more than one muon panel. Fig.8 compares the number of detectors which triggered in coincidence in these 25 muon induced events with those measured during the neutron test.
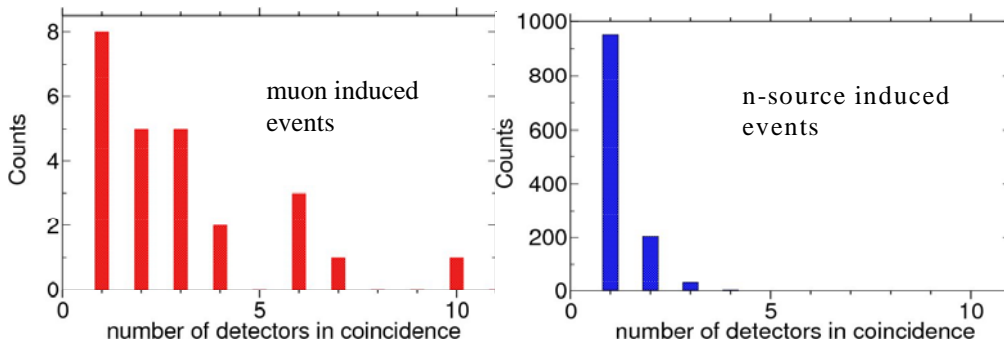
Figure 8: Number of detectors which triggered in coincidence (multiplicity) in events with an oxygen recoil in the signal energy range in at least one of the detectors.

The average multiplicity of the events from the neutron test is much smaller than that of the muon induced neutrons. Most of the coincidences of the neutron test are neutron oxygen scatters in 2 detectors, a few are a neutron oxygen scatter in one detector and a low energy gamma in another, and very few are triple coincidences. Thus, with high probability the event structure of the 2 coincident events in the data is not compatible with that of the neutron test. The muon induced events, on the other hand, are characterized by significantly higher multiplicities and include MeV gammas, similar to the 2 coincident events in the data. The event structure thus clearly suggests that the 2 coincident events in the data are either due to muon induced neutrons not tagged by the veto, or possibly also high energy neutrons which multiplied in the Pb/Cu shields.

It appears therefore justified to use the ratio of *coincident / single*= 17 / 8 = 2.1 of the muon induced neutron events to estimate a single neutron background of 0.94 events in the signal energy range of the oxygen band. This has to be compared to the observed 32 events in this region.

4.2.2 Estimation of alpha background

Fig.9a shows data of the detector with the highest background of degraded alphas in a wide energy range. Besides the discrete alpha lines from alpha emitters in the volume of the crystal one can clearly see a continuum of degraded alphas extending down to energy E=0, very roughly with constant spectral energy density dn/dE.
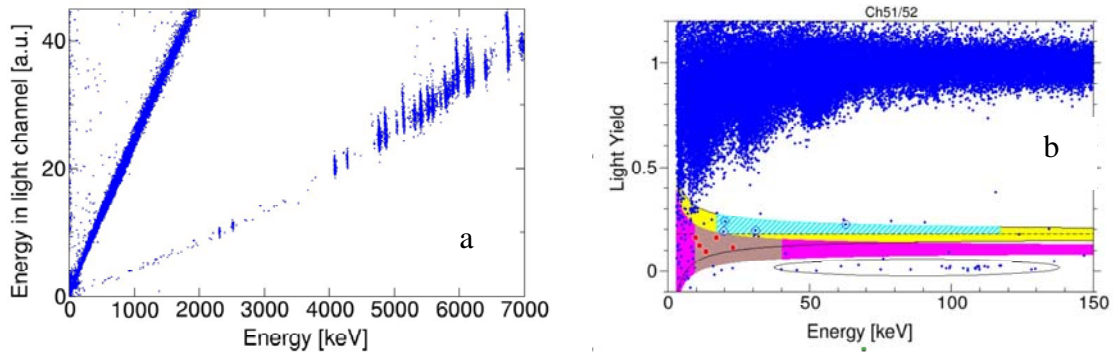
Figure 9a: Detector ch51/52, with the highest background of degraded alphas with continuous energy distribution extending down to energy E=0. The discrete lines are from alpha emitters in the volume of the crystal.

Figure 9b: Low energy event distribution of detector ch51/52 with the highest alpha background. Nuclear recoils from alpha decays are roughly within the elliptical shape. The alpha band is shown in yellow, and alpha events in the cyan dashed region were used to estimate the leakage of alphas into the signal region (brown) of the oxygen band (magenta). Red circles are oxygen recoils in the signal energy range.

Fig.9b shows data of the same detector at lower energies. This detector also has the highest background of Pb recoil nuclei from ^{210}Po alpha decays, clustering around 100 keV. It exhibits a tail that extends down to ~40 keV, further than typically in the other crystals. In addition to the simple process depicted in Fig.4, it is also possible that recoil nuclei from the alpha emitters on the clamps hit the crystal together with some Auger electrons and characteristic X-rays excited by the alpha in the clamp. This process may also add some energy and light and the signal may appear above or in the oxygen band. However, a contamination of the oxygen band by this mechanism very likely occurs at energies above the signal energy range. The alpha band, shown in yellow in Fig.9b, overlaps with the oxygen band at energies below ~60keV and some alpha events may leak into the oxygen band. To estimate the alpha leakage in the signal energy range we use the upper half of the alpha band, above the energy E_{cross}, at which the center of the alpha band intersects with the upper 90% line of the oxygen band. We count the alpha events in the energy range from E_{cross} to E_{cross} + 100 keV in the upper half of the band of each detector (cyan dashed area in Fig.9b) and convert them into a constant spectral energy density dn/dE. With this value of dn/dE, the number of expected alpha events in the signal region is then computed. This estimate gives a total alpha background of 6.9 in the signal region of the oxygen band of all detectors.

4.2.3 Low mass WIMPs

neutron background	0.9
degraded alphas	6.9
gamma leakage	0.9
total	8.7

Table 2: Summary of background estimates in signal energy range of oxygen recoil bands.

Our background estimates are summarized in Table 2. The estimated total background of 8.1 is considerably smaller than the observed 32 events. This excess, when interpreted as dark matter, implies a WIMP mass in the range of ~12 GeV (or less) and an elastic scattering cross section with nucleons of a few times 10^{-5} pb. However we feel that we still have to investigate some questions related to high energy neutrons, and, more importantly, get rid of the alpha related backgrounds before making any kind of definite claim. We are planning a further run with an improved design of the clamps which should completely avoid the alpha related backgrounds. We also plan to roughly double the number of running detector modules in this next run.

4.2.4 Inelastic Dark Matter limits

Inelastic dark matter has been proposed to make a WIMP interpretation of the annual modulation of the rate reported by DAMA/LIBRA compatible with the null results of other experiments. In this model the WIMP has to make a transition to an excited state in order to be

11

able to scatter. This mechanism allows to increase the modulation amplitude and to lower or even suppress the WIMP nucleus scattering rate with light target nuclei. Due to the large mass of the tungsten nucleus, CRESST is very sensitive for inelastic dark matter. Our limits obtained for different mass splittings δ in the relevant range are shown in Fig.10 together with the regions compatible with DAMA. An explanation of the DAMA results with a simple inelastic scattering model is excluded by these results.
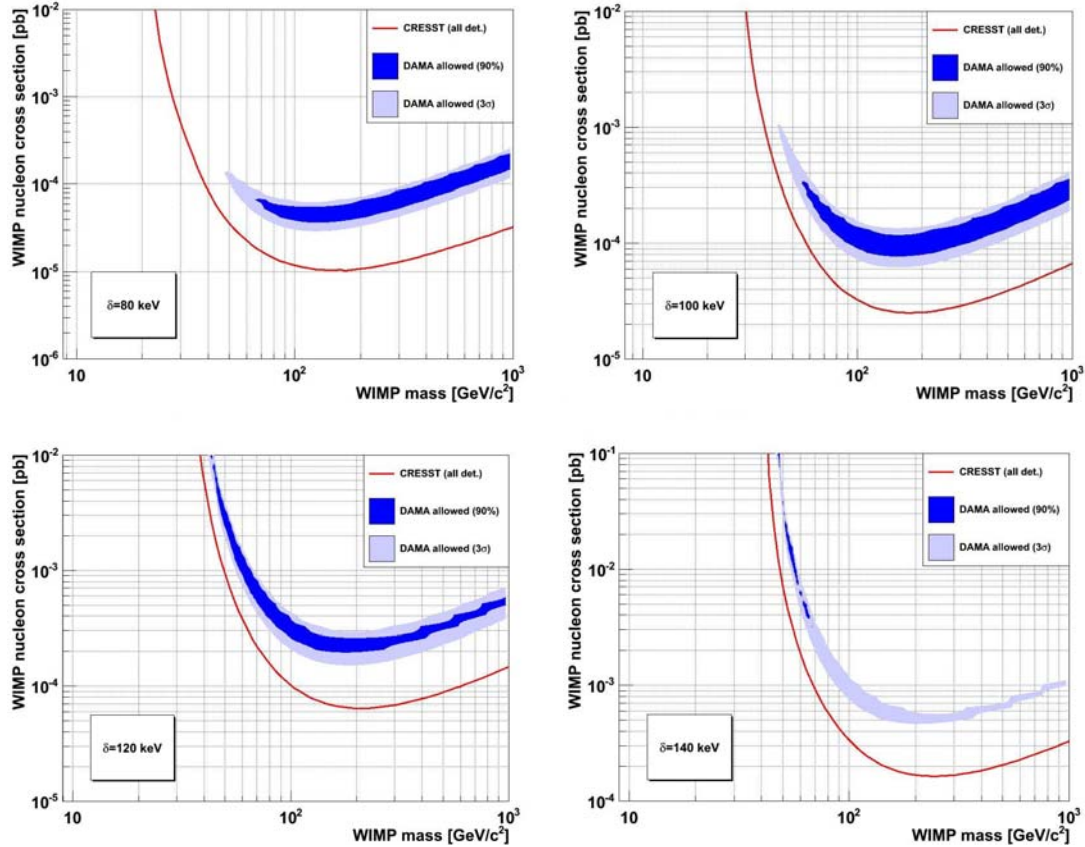
Figure10: Inelastic dark matter limits for mass splittings δ of 80, 100, 120 and 140 keV.

References

[1] I. Bavykina, P. Christ, P. Huff, J. Ninkovic, F. Proebst, W. Seidel and L. Stodolsky, *Interpretation of Light-Quenching Factor Measurements,* Astropart. Phys.**28** (2007) 489

[2] R.F.Lang et al., Scintillator Non-Proportionality and Gamma Quenching in $CaWO_4$, arXiv:0910.4414.

[3] H. Wulandari, et al., Astropart. Phys. **22** (2004) 313

[4] Hesti R.T. Wulandari, PhD Thesis,Technische Universität München, May 2003